Viscous Internal Gravity Waves and Low-Frequency Oscillations in the Tropics

CHIH-PEI CHANG

Department of Meteorology, Naval Postgraduate School, Monterey, Calif. 93940

(Manuscript received 10 January 1977, in revised form 11 March 1977)

ABSTRACT

In this paper we deal with the interpretation of observed oscillations in the tropical troposphere and stratosphere within the framework of the equatorial wave theory. A difficulty with this problem arises when one compares the short vertical wavelength (or equivalent depth) predicted by the classical theory and the observed large vertical scales associated with the low Doppler-shifted frequencies of the tropospheric oscillations. In this analysis it is shown that the inclusion of simple linear damping, justified by budget studies which revealed the important role of cumulus momentum transport, has a strong influence at low frequencies on the forced equatorial waves and results in two types of dispersive relationships. The first type is characteristic of the regular internal gravity waves which have fast phase speeds and weak vertical attenuation. The second type is dominated by the viscous damping time scale and has slow phase speeds and strong vertical trapping. The theory predicts that the stratospheric oscillations may be identified with the first type and the tropospheric oscillations with the second. In the case of Kelvin waves the results can be used to explain consistently both the observed stratospheric Kelvin waves and the planetary-scale Kelvin-like oscillations in the troposphere including the 40–50 day oscillation and the monsoon and Walker circulations. Possible implications with respect to other waves in the tropics are also discussed.

1. Introduction

Based on spectral and cross-spectral analyses of long time series (5–10 years) of tropical station data, Madden and Julian (1971, 1972) detected a global-scale oscillation in the tropical troposphere with a periodicity of 40–50 days. A degree of stationarity of this oscillation in time was also established by them by examining the limited amount of station pressure data available from the 1890's. Their results indicate that this oscillation is most prominent in the zonal velocity component and the surface pressure, with the maximum amplitude situated along the equator. There are some time and spatial variations within a 40–50 day cycle as depicted in Fig. 1 which is reproduced from a schematic diagram constructed by Madden and Julian (1972), but basically the oscillation propagates eastward at a fairly steady phase speed and, at most times, exhibits a zonal wavenumber 1 structure. Madden and Julian (1972) argued that enhanced deep cumulus convection is usually associated with large-scale upward motion and the oscillation appears as two vertical circulation cells along the equatorial zonal plane.

The above structure resembles that of a theoretical atmospheric Kelvin wave (Holton and Lindzen, 1968) in several ways: the direction of propagation, the meridional structure and the absence of large amplitude in the meridional wind component. However, for a given phase speed as slow as that observed, Kelvin wave theory would predict a fairly short vertical wavelength which does not appear to agree with that of the observed oscillation. This discrepancy, which has been a major difficulty for the theoretical understanding of the 40–50 day oscillations, has also been encountered by several meteorologists in their efforts to interpret various types of large-scale tropical wave motions using the equatorial wave theory. In a linear analysis Lindzen (1967) has shown that for synoptic (and larger) time scales, waves on an equatorial beta-plane generally propagate in the vertical as internal gravity waves with rather short vertical wavelengths. This result was evident in a study of the response of the tropical atmosphere to stationary heating by Webster (1972, 1973). In a two-level (750 and 250 mb) numerical model he found that the equatorial response in an easterly basic current has a horizontal structure that is characteristic of Kelvin waves. However, his analytical solution for the case of an idealized basic flow possesses very short vertical wavelength [$\sim O(1$ km)] and appears to suggest that higher vertical resolution is required for the numerical model.

The short vertical wavelength predicted by the equatorial wave theory arises from the internal gravity wave character of these waves. Since for pure gravity waves the phase speed c is given by $c=(gh)^{\frac{1}{2}}$, where

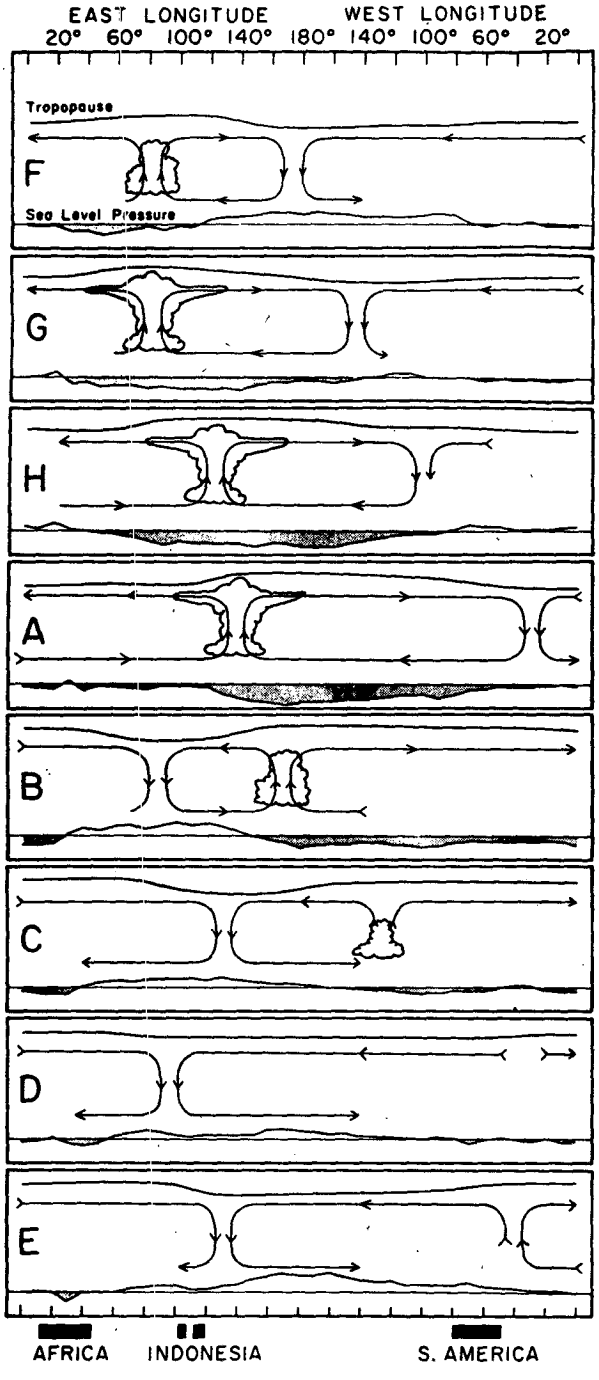

FIG. 1. Schematic depiction of the time and space (zonal plane) variations of the circulation cells associated with the 40–50 day oscillation. The mean pressure disturbance is plotted at the bottom of each chart with negative anomalies shaded. Regions of enhanced large-scale convection are indicated schematically by the cumulus and cumulonimbus clouds. The relative tropopause height is indicated at the top of each chart. (From Madden and Julian, 1972.)

g is the gravitational constant and h a depth scale for the motion (usually called the equivalent depth), the vertical wavelength tends to be proportional to the phase speed. Within the range of large-scale tropical motions in the tropical troposphere the phase speed is usually slow compared to the external gravity wave phase speed, so the vertical wavelength is consequentially small compared to that given by the scale height. The observed Kelvin waves (Wallace and Kousky, 1968) and mixed Rossby-gravity waves (Yanai and Maruyama, 1966) in the lower stratosphere have rather large Doppler-shifted phase speeds (relative to the mean zonal wind) so that their observed vertical wavelengths are in better agreement with the theory. In Table 1 we summarize the comparison between the observed vertical wavelengths and that given by the equatorial wave theory for three major zonal wind oscillations in the tropics: the stratospheric Kelvin wave, the 40–50 day oscillation and the planetary-scale stationary motion which could include the east–west overturning Walker circulation along the equatorial plane (Bjerknes, 1969; Webster, 1973) or the winter monsoon (Krishnamurti *et al.*, 1973; Webster, 1973). The theoretical vertical wavelength is calculated using the Doppler-shifted phase speed with the mean zonal flow specified by an averaged tropospheric easterly speed of -5 m s^{-1}. This specification is based on the evidence that all these oscillations, including the stratospheric Kelvin wave, are generated by energy sources in the troposphere.

The equatorial wave theory used in Table 1 is basically inviscid because it does not include a significant frictional effect in the free atmosphere. In a numerical diagnostic study of the seasonal-mean circulation at 200 mb during the northern summer, Holton and Colton (1972) found that a very strong damping term (corresponding to linear damping time scale of $\sim$1 day) is needed in the linearized barotropic vorticity equation to balance the generation of planetary-scale vorticity by horizontal divergence. Since the planetary-scale divergence field is largely a result of the strong condensation heating in the middle troposphere due to the vigorous cumulus convection associated with the summer monsoon, Holton and Colton hypothesized that the vertical mixing of vorticity and momentum by cumulus convection could account for this strong damping. This hypothesis is also consistent with several budget studies of synoptic-scale, cumulus-related tropical motions (Reed and Recker, 1971; Williams and Gray, 1973; Reed and Johnson, 1974; Chu, 1976; and others), and the numerical diagnostic study by Chang *et al.* (1975). Recently Stevens *et al.* (1977) also show that this strong damping mechanism is responsible for reducing the theoretically calculated amplitude of the tropical waves forced by heating to the observed magnitude. Thus the inclusion of this mechanism in the equatorial wave theory seems to be necessary for the proper

TABLE 1. Comparison of observed tropical zonal oscillations and the inviscid equatorial wave theory. The theoretical vertical wavelengths are based on the observed Doppler-shifted phase speeds which assume a basic zonal wind of $\bar{u}=-5$ m s^{-1}. See text for details.

	Observations					Theory
Oscillations	Period (days)	Zonal wavenumber	Ground phase speed (m s^{-1})	Doppler-shifted* phase speed (m s^{-1})	Vertical wavelength (km)	Vertical wavelength (km)
Stratospheric Kelvin waves (Wallace and Kousky, 1968)	10-15	1-2	25-45	30-50	10-15(strat) 17-26(tropo)	17-29
40-50 day oscillations (Madden and Julian, 1972)	40-50	1	9-11	14-16	15-30	8-9
Stationary planetary circulations (monsoon and Walker)	∞	1-2	0	5	15-30	3

* $\bar{u}=-5$ m s^{-1}.

interpretation of the observed tropical motions forced by cumulus heating.

The purpose of this paper is to study the effect of the strong damping mechanism called for by previous budget studies on tropical wave dynamics. The simplest form of linear drag will be used to represent this effect as was done by Holton and Colton (1972). We will show that this effect in some cases is more than just an expected reduction in the amplitude of the thermally forced waves or a near-trivial correction in the frequency equation. Moreover, in these cases it can account for most of the discrepancies in Table 1 and provide a consistent theoretical basis for the interpretation of the tropical oscillations in both the stratosphere and the troposphere.

2. Basic equations

Since the vertical structure equation of all equatorial waves is identical to that for two-dimensional gravity waves, we will consider only the Kelvin wave case for the purpose of simplicity. Setting the meridional velocity zero we may write the linearized zonal momentum, meridional momentum, hydrostatic, thermodynamic energy and continuity equations on an equatorial beta-plane, with a single zonal wavenumber k and constant phase speec c relative to the basic zonal flow as

$$-ikcu=-ik\phi-Du, \tag{1}$$

$$\beta yu=-\frac{\partial\phi}{\partial y}, \tag{2}$$

$$\frac{\partial\phi}{\partial z}=\frac{RT}{H}, \tag{3}$$

$$-ikcT+w\Gamma=\frac{Q}{c_p}-DT, \tag{4}$$

$$iku+e^{z/H}\frac{\partial}{\partial z}(e^{-z/H}w)=0, \tag{5}$$

where u, w, T, ϕ and Q are the perturbation zonal velocity, vertical velocity, temperature, geopotential and the diabatic heating rate, respectively; H is a constant scale height, Γ the static stability, c_p the specific heat at constant pressure, R the gas constant, β the meridional gradient of the vertical component of earth's vorticity, y the meridional coordinate; and $z=-H\ln(p/p_0)$ is the vertical coordinate with p the pressure and p_0 a reference pressure. The damping effect is represented by the linear drag coefficient D in the zonal momentum equation. A Newtonian cooling term with the same coefficient is included in the thermodynamic energy equation in order to facilitate the analysis.

Eqs. (1)-(2) give the meridional structure of the Kelvin waves:

$$u,\phi\propto\exp(-\beta y^2/2\hat{c}), \tag{6}$$

where

$$\hat{c}\equiv c+iD/k,$$

and the condition $\mathrm{Re}(\hat{c})=c>0$ is required to satisfy the trapping condition on an equatorial β-plane. If a height-dependence factor, $\exp(z/2H)$, is separated from the perturbation quantities, Eqs. (1) and (3)-(5) may be combined to form a single equation in w:

$$\frac{\partial^2 w'}{\partial z^2}+\lambda^2 w'=\frac{Q'}{\hat{c}^2}, \tag{7}$$

where

$$\lambda^2 \equiv \frac{S}{\hat{c}^2} - \frac{1}{4H^2}, \tag{8}$$

$$w' \equiv we^{-z/(2H)},$$

$$Q' \equiv \frac{R}{c_p H} Qe^{-z/(2H)},$$

$$S \equiv \frac{R}{H}\Gamma.$$

The parameter λ is a measure of the vertical wavenumber. If the heating function Q' is given, (7) can be solved with suitable boundary conditions. In our problem the following boundary conditions are used:

$$w = \begin{cases} 0, & \text{at } z=0 \quad (9a) \\ C_1 e^{i\lambda z} + C_2 e^{-i\lambda z}, & \text{at } z=z_t \quad (9b) \end{cases}$$

where

$$C_1 = rC_2.$$

Here z_t is the height of tropopause and the condition (9b) results from the requirement that latent heating vanishes at z_t. The parameter r is a reflection coefficient which, in the absence of vertical wind shear, is given by the model specification of the static stability distribution. The solution to (7) may be written in the form

$$w(z) = -\frac{re^{i\lambda z} + e^{-i\lambda z}}{\lambda(1+r)} \int_{z_c}^{z_t} \sin\lambda z \frac{Q'}{gh} dz, \quad z \geqslant z_t, \tag{10a}$$

$$w(z) = -\frac{\sin\lambda z}{\lambda(1+r)} \int_{z}^{z_t} (re^{i\lambda z} + e^{-i\lambda z}) \frac{Q'}{gh} dz - \frac{re^{i\lambda z} + e^{-i\lambda z}}{\lambda(1+r)} \times \int_{z_c}^{z} \sin\lambda z \frac{Q'}{gh} dz, \quad z_t > z > z_c, \tag{10b}$$

$$w(z) = -\frac{\sin\lambda z}{\lambda(1+r)} \int_{z_c}^{z_t} (re^{i\lambda z} + e^{-i\lambda z}) \frac{Q'}{gh} dz, \quad z_c \geqslant z \geqslant 0. \tag{10c}$$

Here z_t is the height of cloud top and z_c the height of cloud base. Chang (1976) has used the above equations to show that, in the case of $D=0$, the vertical energy flux of Kelvin waves due to pressure work is

$$\overline{\phi' w'} \approx \frac{S^{\frac{1}{2}}}{k} \overline{w'^2}, \tag{11}$$

where the overbar denotes the zonal average and $\phi' = \phi \exp(-z/2H)$. Eqs. (11) and (7) indicate that for this case the upward forcing of Kelvin waves is most efficient for long waves. Augmented by the fact that waves with a vertical scale equal to twice that of forcing are most efficiently excited (Green, 1965 and Lindzen, 1966), Chang (1976) was able to show that the Kelvin wave response given by the inviscid theory agrees with the observed stratospheric Kelvin waves.

If we consider downward phase propagation (upward energy propagation) only, $\mathrm{Re}(\lambda) > 0$. For $H \sim 7$ km and vertical wavelength $\ll 88$ km, Eq. (8) may be approximated by

$$\hat{c}\lambda = S^{\frac{1}{2}}. \tag{12}$$

In the inviscid case, $D=0$ and $\hat{c}=c$ so that λ is pure real. In the case of $D \neq 0$, $\hat{c} = c_r + ic_i$ where $c_r = c > 0$ and $c_i = D/k > 0$; thus λ becomes complex, i.e., $\lambda = \lambda_r + i\lambda_i$. Here λ_i describes the exponential increase ($\lambda_i > 0$) or decrease ($\lambda_i < 0$) of the amplitude with height. Eq. (12) now becomes quadratic and has the following roots:

$$c_{rI,II} = \frac{S^{\frac{1}{2}} \pm (S - 4\lambda_r^2 c_i^2)^{\frac{1}{2}}}{2\lambda_r} > 0, \tag{13}$$

$$\lambda_{iI,II} = \frac{-S^{\frac{1}{2}} \pm (S - 4\lambda_r^2 c_i^2)^{\frac{1}{2}}}{2c_i} < 0. \tag{14}$$

The subscripts I and II are being used to denote the plus and minus roots, respectively. It is obvious that $c_{rI} > c_{rII}$ and $|\lambda_{iI}| < |\lambda_{iII}|$, hence the first solution (which shall be called Mode I) has a fast horizontal phase speed and can propagate more efficiently into higher levels while the second solution (Mode II) is slower and attenuates faster above the source region. In addition, Eqs. (13) and (14) indicate that the waves are excitable only if

$$\lambda_r < \frac{S^{\frac{1}{2}}}{2c_i} \left(= \frac{kS^{\frac{1}{2}}}{2D} \right), \tag{15}$$

so that the effect of damping causes a short-wave cutoff in the vertical or a long-wave cutoff in the horizontal.

If we take the inviscid limit of $D \to 0$, Eqs. (13) and (14) reduce to

$$\left.\begin{aligned} c_{rI} &= S^{\frac{1}{2}}/\lambda_r \\ \lambda_{iI} &= 0 \end{aligned}\right\}. \tag{16}$$

$$\left.\begin{aligned} c_{rII} &= 0 \\ \lambda_{iII} &= -\infty \end{aligned}\right\}. \tag{17}$$

Comparing (16) and (12) it is seen that Mode I corresponds to the regular inviscid solution. Substituting (17) into (1)–(5) leads to a trivial solution of vanishing wave amplitude. Thus Mode I may be called the "regular mode" and Mode II the "viscous mode," because the latter is non-trivial only when $D \neq 0$.

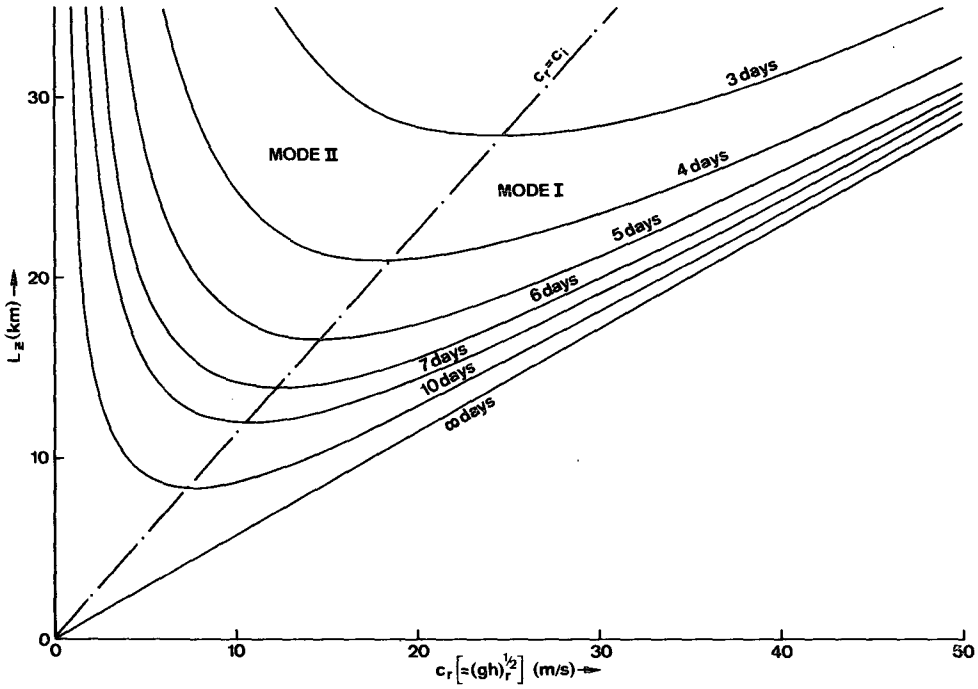

FIG. 2. Real Doppler-shifted phase speed c_r as a function of vertical wavelength L_z and damping time. For the convenience of application to other types of equatorial waves, the abscissa can also be designated by $(gh)_r^{\frac{1}{2}}$, where h is the equivalent depth.

Fig. 2 shows the real phase speed c_r as a function of vertical wavelength $L_z(=2\pi/\lambda_r)$ and the viscous damping time scale $1/D$. For $D=0$ (damping time scale ∞) the dispersion relationship of Mode I is a straight line of $c_r \propto L_z$, typical of the internal gravity waves. In addition, the vertical coordinate ($c_r=0$) represents the trivial solution of Mode II. For $D\neq 0$ the two modes are represented by the quadratic curves. The effect of damping on Mode I is a relatively small modification with L_z increasing as c_r increases. The modification for Mode II is more substantial and L_z generally decreases as c_r increases. The two modes are separated by the line $c_r=c_i$. For Mode I $c_r>c_i$, i.e., the inertial time scale is faster than the damping time scale. The reverse is true for Mode II.

The imaginary vertical wavenumber λ_i is shown in Fig. 3 as a function of vertical wavelength and damping time scale. Here the magnitude of λ_i decreases with increasing L_z for Mode I and increases with L_z for Mode II. The $c_r=c_i$ curve again provides the partition of the two modes.

From Figs. 2 and 3 it can be seen that, if a certain vertical wavelength is most efficiently excited by a given forcing function, both modes will be excited for $D\neq 0$. The regular mode will have fast zonal phase speed and less vertical attenuation, while the viscous mode will have slow zonal phase speed and is more trapped in the vertical away from the source region.

3. Response of specified heating

The Kelvin wave response of the tropical atmosphere can be calculated if the vertical heating function Q' in (7) is known. As in Chang (1976) we will use the vertical heating profile

$$Q' \propto Sq(y)\sin\pi\left(\frac{z-z_c}{\Delta z}\right), \quad z_t \geqslant z \geqslant z_c$$

$$Q'=0, \qquad z>z_t \text{ or } z<z_c$$

where the function $q(y)$, which specified the meridional distribution of heating, is assumed to take the form of (6). Solution (10) will be evaluated by specifying the vertical scale of the heating $\Delta z \equiv z_t - z_c = 14$ km, $D=2.3\times 10^{-6}$ s^{-1} (damping time $=5$ days) and $S_s=3S_t$, where S_s and S_t are the static stability for the stratosphere and troposphere, respectively.

Since Mode I is less trapped in the vertical we expect that it may be more prominent away from the source region. Using (10a) we display the vertical wave energy flux due to pressure work, $\overline{\phi' w'}$, at z_t as a function of vertical wavelength L_z and zonal wavenumber $s(=ka$, where a is the radius of the earth), in Fig. 4. The cross-hatched area in the lower part of the diagram indicates the short vertical wavelength cutoff required by (15). The maximum response occurs at zonal wavenumber 1–2 and vertical wavelength 30–35 km. As expected, this result is similar to that

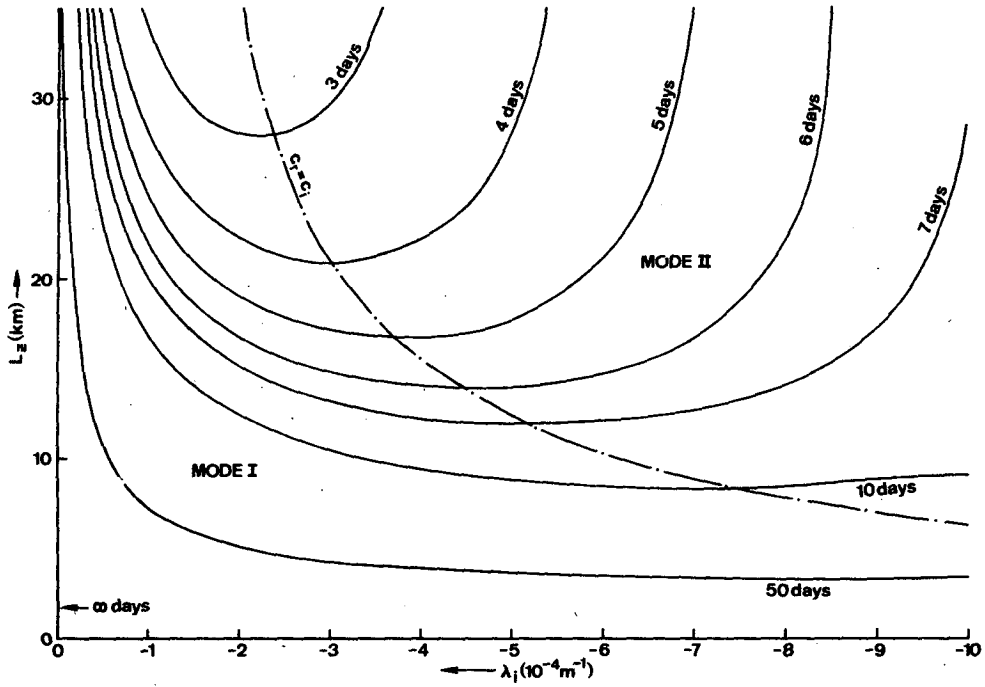

FIG. 3. Imaginary vertical wavenumber λ_i as a function of vertical wavelength and damping time.

obtained by Chang (1976) except that the vertical wavelength is slightly longer and wavenumber 2 becomes comparable in importance to wavenumber 1. This vertical wavelength range, according to Fig. 2, implies a Doppler-shifted phase speed $\sim$50 m s^{-1}, in reasonable agreement with the observed stratospheric Kelvin waves.

For the highly trapped Mode II the vertically-integrated tropospheric kinetic energy is considered an appropriate measurement for the response spectrum. Fig. 5 shows this quantity as a function of L_z and s. Here the zonal scale selection clearly favors the lowest zonal wavenumber, but all vertical wavelengths beyond the short-wave cutoff have about the same response. Thus the most prominent viscous mode excited should be of zonal wavenumber 1 and vertical wavelength $\gtrsim$17 km. For vertical wavelength $\sim$17 km the Doppler-shifted phase speed is $\sim$10 m s^{-1} according to Fig. 2. These values agree quite well with the 40–50 day oscillation observed by Madden and Julian

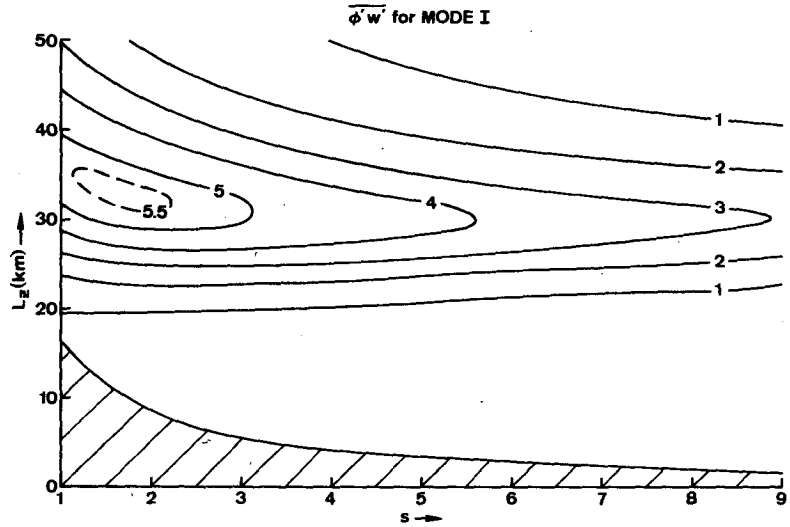

FIG. 4. Vertical wave energy flux due to pressure work at the tropopause level, $\overline{\phi' w'}$, as a function of vertical wavelength L_z and zonal wavenumber s for Mode I. Units are arbitrary.

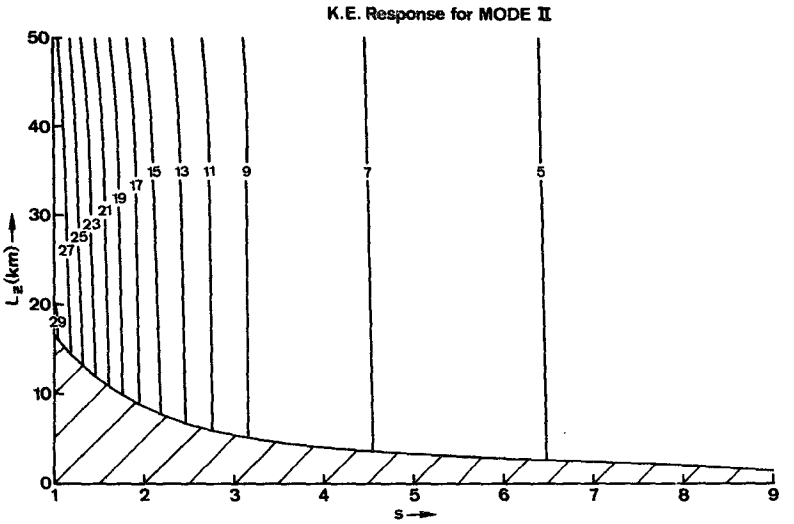

FIG. 5. Tropospheric kinetic energy response for Mode II as a function of vertical wavelength and zonal wavenumber. Units are arbitrary.

(1972). However, if the forcing function has a white noise distribution in frequency the maximum Mode II response is still somewhat smaller than the maximum Mode I response. The absence of detectable 10–15 day Kelvin waves in the troposphere therefore indicates that the thermal forcing is of a red noise nature. However, this requirement of red noise distribution is not so much for the explanation of the stratospheric Kelvin waves, as suggested by Holton (1973); rather, it is for the explanation of the dominance of low-frequency oscillations in the troposphere. The 10–15 day Kelvin waves in this case are of relatively higher frequencies and can become prominent only above the troposphere where the lower frequency viscous mode is greatly attenuated.

The above results are summarized in Table 2 within the "non-resonant selection" category. The stationary waves related to the Walker circulation or the winter monsoon may, on the other hand, be viewed as due to resonant excitation by the stationary heat sources, because the forcing function has a pre-selected zero ground phase speed. By assuming a zonal mean wind of -5 m s^{-1} in the source region the Doppler-shifted phase speed of this resonance is 5 m s^{-1}. Referring back to Fig. 2, response is possible only in the Mode II regime with a vertical wavelength of $\sim$27 km for the case of 5-day damping time. This vertical wavelength agrees much better with the observed monsoon or Walker circulation than Webster's (1972) inviscid calculation of $\sim$1 km. In addition, Fig. 5 still indicates that zonal wavenumber 1 should be clearly preferred over shorter waves if the heat source has a white noise distribution in the zonal scales. In the real atmosphere the differential heating due to land-sea differences, as in the case of monsoon, or due to sea-surface temperature variations, as in the case of Walker circulation, is usually confined to lower zonal wavenumbers; so it is not surprising to observe the large zonal scale of these circulations. On the other hand, Egger (1976) reported that the response to the imposed heating anomalies in a linear model almost always favors the lowest wavenumbers regardless of the zonal scale of the anomaly imposed on the model. His experimental result is entirely understandable in

TABLE 2. The most efficiently excited Kelvin waves predicted by the viscous theory.

		Vertical wavelength (km)	Zonal wavenumber	Doppler-shifted phase speed (m s^{-1})	Ground phase speed (m s^{-1})
Resonant selection	Mode I	31–35	1–2	50–58	45–53
	Mode II	$\gtrsim$17	1	15	$\gtrsim$10
Non-resonant selection	Mode I	(not excitable)			
	Mode II	27	1	5	0

Damping time = 5 days.
Vertical scale of heating = 14 km.

view of our result. This low-wavenumber preference for the thermally forced Kelvin wave response is related to (11) and the explanation has been given by Webster (1973) and Chang (1976).

4. Further comparison with the 40–50 day oscillation

As mentioned previously, the two solutions of (12) are separated by the curve $c_r=c_i$. Since for Mode I the inertial time scale is faster than the damping time scale, it follows that the main balance in Eq. (1) is between the first two terms, i.e.,

$$-ikcu\approx ik\phi.$$

In this case u and ϕ are in-phase and the wave is characteristic of the internal gravity waves. For Mode II the damping time scale is faster so that the main balance is between the last two terms, i.e.,

$$0=-ik\phi-Du.$$

Thus u and ϕ have a quarter-cycle phase difference which is characteristic of a highly viscous wave motion. If we examine the schematic diagram of the 40–50 day oscillation (Fig. 1) depicted by Madden and Julian, it can be seen that, for most of the categories, u and ϕ have a phase relationship between in-phase and quarter-cycle difference. The important effect of damping is thus clearly indicated.

If the vertical scale is large, the main balance in the thermodynamic energy equation is between the adiabatic cooling and the diabatic heating. The residue is approximately balanced by the advective term for Mode I, i.e.,

$$-ikcT\approx\frac{Q}{c_p}-w\Gamma$$

and T, w will have a quarter-cycle phase difference. For Mode II this residue is mainly balanced by the damping term, i.e.,

$$w\Gamma-\frac{Q}{c_p}\approx DT.$$

In this case T, w will be in-phase if diabatic heating exceeds adiabatic cooling and half-cycle out-of-phase if adiabatic cooling dominates over diabatic heating. In Madden and Julian's (1972) observational study they found that the surface pressure is half-cycle out-of-phase with the 300 mb temperature and in-phase with the 100 mb temperature. Since vertical motion is close to in-phase with surface pressure as shown by Fig. 1, it may be inferred that T and w are in-phase at 300 mb and half-cycle out-of-phase at 100 mb. The former level is in the upper troposphere where diabatic heating must dominate for the motion to be self-sustaining, while the latter level is near the tropopause where the diabatic heating vanishes but the vertical motion may overshoot through the cloud top. The thermal structure of the 40–50 day oscillation thus also appears to be consistent with the viscous theory.

When damping is included, the meridional structure of the Kelvin waves as expressed by (6) contains a tilt of the wave axis because $\hat{c}$ is complex, i.e.,

$$\exp\left(-\frac{\beta y^2}{2\hat{c}}\right)=\exp\left(-\frac{\beta}{2}\frac{c_r}{c_r^2+c_i^2}y^2\right)\exp\left(i\frac{\beta}{2}\frac{c_i}{c_r^2+c_i^2}y^2\right)$$

$$=\exp\left(-\frac{\beta\lambda_r}{2S^{\frac{1}{2}}}y^2\right)\exp\left(i\frac{\beta\lambda_r c_i}{2S^{\frac{1}{2}}c_r}y^2\right). \qquad (18)$$

Here the first part of the right-hand side gives a Gaussian distribution in the meridional direction with a Gaussian folding with y_G given by

$$y_G=\left(\frac{2S^{\frac{1}{2}}}{\beta\lambda_r}\right)^{\frac{1}{2}}=\left(\frac{2}{\beta}c_r|_{D=0}\right)^{\frac{1}{2}}.$$

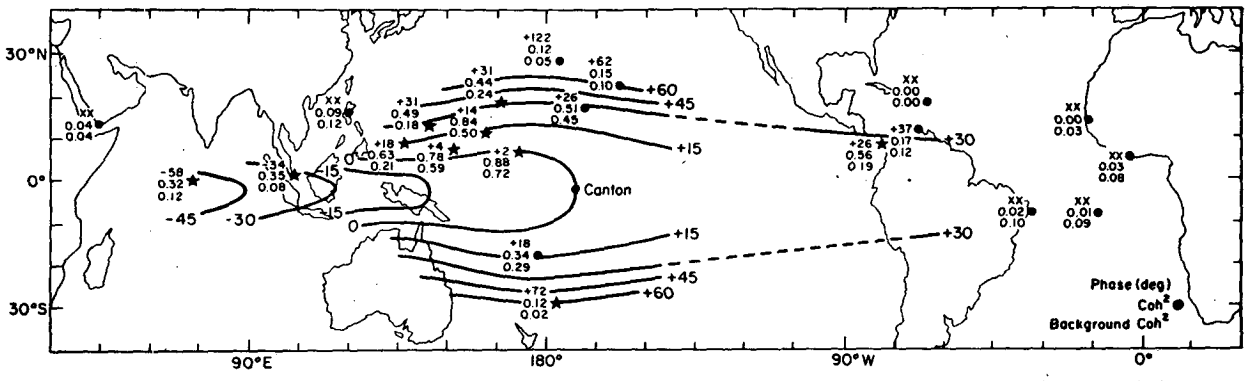

FIG. 6. Mean phase angles, coherence-squares and background coherence-squares for approximately the 36–50 day period range of cross spectra between all stations and Canton. The plotting model is given in lower right-hand corner. Positive phase angles at a station means the Canton series leads that of the station. Stations indicated by a star have coherence-squares above the background at the 95% level. Mean coherence-squares at Shemya (52°43'N, 174°6'E) and Campbell I. (52°33'S, 169°9'E) [not shown] are 0.08 and 0.02, respectively. Both are below their average background coherence-squares. (From Madden and Julian, 1972.)

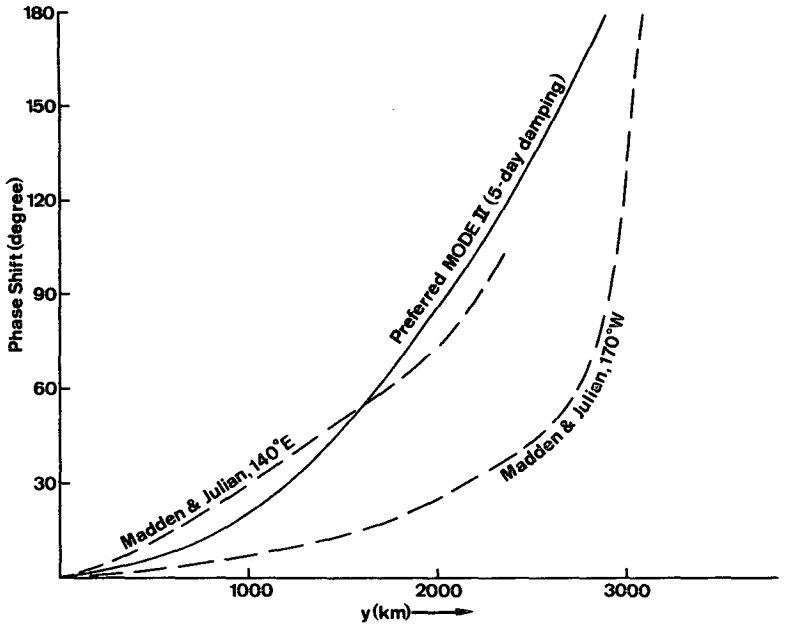

FIG. 7. Comparison of the meridional phase tilt of the 40–50 day oscillation at 140°E, 170°N, observed by Madden and Julian (1972), and the value of the most efficient Mode II response predicted by the viscous theory.

This meridional trapping scale is identical for both the regular and the viscous modes for a given vertical wavelength. In the case of the most efficient Mode II response discussed in the previous section, $|y_G| = 1500$ km and agrees quite well with the observed 40–50 day oscillation. The second part of the right-hand side of (18) gives rise to a periodic variation of the waves in y^2, and therefore a meridional tilt of the wave axis. It also implies a poleward phase propagation for the Kelvin waves because $c_r>0$, $c_i>0$ and $\lambda_r>0$.

A strong meridional tilt was found by Madden and Julian for the 40–50 day oscillation using cross-spectral analysis of the surface pressure data. Their phase diagram, constructed by using the Canton Island series as the base series, is reproduced here in Fig. 6. Although the meridional phase tilt seems to vary in different geographical locations, near Canton Island and near the equator the tilt is primarily NW–SE north of the equator and NE–SW south of the equator. For eastward propagating waves this indicates a poleward phase propagation. In Fig. 7 the phase tilt of the 40–50 day oscillation deduced from Fig. 6 at two different longitudes, 170°W (near Canton Island) and 140°E (active convection area in Indonesia), are plotted along with that given by the viscous theory. Within the limitation of our simple theory and the approximations invoked, the theoretical result can be considered as fairly good in simulating the observed phase tilts.

5. Concluding remarks

We have shown that the inclusion of a damping term can result in two types of dispersive relationships for the forced Kelvin waves. The first type (Mode I) is characteristic of the regular internal gravity waves which propagate rapidly in the zonal direction and attenuate slowly in the vertical. The second type (Mode II) is dominated by the viscous damping time scale and has slower zonal phase speed and faster vertical attenuation. This viscous mode reduces to a trivial solution in the inviscid limit so its existence is supported only by damping. Assuming that the main thermal sources in the tropics are confined to the troposphere and have a red noise distribution which enhances the response of the viscous mode, this theory predicts that the stratospheric waves behave like the regular mode and the tropospheric waves behave like the viscous mode. Our theory includes features that are consistent with several results found by previous theoretical or numerical studies of the equatorial waves that incorporate the damping mechanism. Lindzen (1971) and Holton and Lindzen (1972) found that as a wave is propagating in weak vertical wind shear, the efficiency of damping would change inversely according to the change of the Doppler-shifted phase speed. This is consistent with our result that the slower moving waves are more trapped in the vertical. In a numerical diagnostic model of the Kelvin waves, Holton (1973) observed a maximum response in the tropospheric wavenumber 1 spectrum with period >30 days. This response

seems to correspond to our viscous mode. Very recently Stevens *et al.* (1977) reported that with a parameterization of the cumulus damping, the tropical waves have very little vertical structure. This is again explainable by our theory because the vertical wavelength is increased as a result of damping.

In real atmosphere the damping due to cumulus convection and other processes is much more complicated than the simple linear drag term used in our analysis. However, the agreement with observed zonal wind oscillations such as the stratospheric Kelvin waves, the 40–50 day oscillations, and the stationary monsoon and Walker circulations strongly indicate that our theoretical interpretation is quite relevant to these oscillations. In addition, although the present analysis is limited to Kelvin waves only, the vertical structure equation applies to all equatorial waves. Hence it would be quite possible that the general result also applies to other thermally controlled tropical wave disturbances. This is particularly interesting in view of the large vertical scale and slow Doppler-shifted phase speed usually observed in the tropical tropospheric waves such as the easterly waves. In a discussion of the present results, Wallace (personal communication) suggested that they would also explain the seemingly non-dispersive westward propagation of the synoptic-scale cloud clusters observed in the time sections of tropical satellite pictures (Chang, 1970). In these sections the propagating cloud patterns have quite uniform phase speeds but the apparent wavelength varies over a large range. This non-dispersive character led Wallace (1972) to propose that, despite the strong vertical and longitudinal variations of the basic flow, they are more likely a result of advection by basic flow than a manifestation of some kind of Rossby waves. He argued that the difficulty of ascertaining a steering level is not as severe as that of explaining why the beta-effect does not produce dispersive phase speeds. However, to interpret these patterns as being passive cloud masses advected by the basic flow is also unsatisfactory due to the fact that they are frequently observed to be associated with active convections and that they sometimes decay and regenerate during the course of propagation. These difficulties are partially alleviated in the framework of the present theory because the viscous mode should have a much smaller Doppler-shifted phase speed and would appear as if they are advected by the basic easterly current at some levels.

Acknowledgments. The author wishes to thank Professors J. R. Holton, P. J. Webster and J. M. Wallace for discussion and Professors R. T. Williams and G. J. Haltiner for reading the manuscript. This work was supported by the Atmosphere Research Section, National Science Foundation, under Grant DES 75-10719.

REFERENCES

Bjerknes, J., 1969: Atmospheric teleconnections from the equatorial Pacific. *Mon. Wea. Rev.*, **97**, 163–172.

Chang, C.-P., 1970: Westward propagating cloud patterns in the tropical Pacific as seen from time-composite satellite photographs. *J. Atmos. Sci.*, **27**, 133–138.

——, 1976: Forcing of stratospheric Kelvin waves by tropospheric heat sources. *J. Atmos. Sci.*, **33**, 740–744.

——, F. T. Jacobs and B. B. Edwards, 1975: A diagnostic model for estimating large-scale flow patterns in the tropical upper troposphere from satellite cloud brightness data. *Mon. Wea. Rev.*, **103**, 536–549.

Chu, J.-H., 1976: Vorticity in maritime cumulus clouds and its effects on the large-scale budget of vorticity in the tropics. Ph.D. thesis, University of California, Los Angeles, 123 pp.

Egger, J., 1976: The linear response of the atmosphere to sea surface temperature anomalies in the tropical Pacific. Paper presented at the JOC Study Conference on Numerical Modelling for the Tropics, Exeter, England. [Available from Meteorologisches Institut, Der Universität, Munchen, Theresienstrasse 37, D8000 Munchen 2, FRG.]

Green, J. S. A., 1965: Atmospheric tidal oscillations: An analysis of the mechanics. *Proc. Roy. Soc. London*, **A288**, 564–574.

Holton, J. R., 1973: On the frequency distributions of atmospheric Kelvin waves. *J. Atmos. Sci.*, **30**, 499–501.

——, and D. E. Colton, 1972: A diagnostic study of the vorticity balance at 200 mb in the tropics during the northern summer. *J. Atmos. Sci.*, **29**, 1124–1128.

——, and R. S. Lindzen, 1968: A note on "Kelvin" waves in the atmosphere. *Mon. Wea. Rev.*, **96**, 385–386.

——, and ——, 1972: An updated theory for the quasi-biennial cycle of the tropical stratosphere. *J. Atmos. Sci.*, **29**, 1076–1080.

Krishnamurti, T. N., Kanamitsu, W. J. Koss and J. D. Lee, 1973: Tropical east–west circulations during the northern winter. *J. Atmos. Sci.*, **30**, 780–787.

Lindzen, R. S., 1966: On the relation of wave behavior to source strength and distribution in a propagating medium. *J. Atmos. Sci.*, **23**, 630–632.

——, 1967: Planetary waves on beta planes. *Mon. Wea. Rev.*, **95**, 441–451.

——, 1971: Equatorial planetary waves in shear: Part I. *J. Atmos. Sci.*, **28**, 609–622.

Madden, R. A., and P. R. Julian, 1971: Detection of a 40–50 day oscillation in the zonal wind in the tropical Pacific. *J. Atmos. Sci.*, **28**, 702–708.

——, and ——, 1972: Description of global-scale circulation cells in the tropics with a 40–50 day period. *J. Atmos. Sci.*, **29**, 1109–1123.

Reed, R. J., and R. H. Johnson, 1974: The vorticity budget of synoptic-scale wave disturbances in the tropical western Pacific. *J. Atmos. Sci.*, **31**, 1784–1790.

——, and E. E. Recker, 1971: Structure and properties of synoptic-scale waves in the equatorial western Pacific. *J. Atmos. Sci.*, **28**, 1117–1133.

Stevens, D. E., R. S. Lindzen and L. Shapiro, 1977: A new model of tropical waves incorporating momentum mixing. Submitted to *Dynamics of Atmospheres and Oceans.*

Wallace, J. M., 1972: On the general circulation of the tropics. Dynamics of the tropical atmosphere. NCAR Summer Colloquium Notes, 192–193. [Available from Advanced Study Program, NCAR.]

——, and V. E. Kousky, 1968: Observational evidence of Kelvin waves in tropical stratosphere. *J. Atmos. Sci.*, **25**, 900–907.

Webster, P. J., 1972: Response of the tropical atmosphere to local steady forcing. *Mon. Wea. Rev.*, **100**, 518–541.

——, 1973: Temporal variation of low-latitude zonal circulations. *Mon. Wea. Rev.*, **101**, 803–816.

Williams, K. T., and W. M. Gray, 1973: Statistical analysis of satellite-observed trade wind cloud clusters in the western North Pacific. *Tellus*, **25**, 313–336.

Yanai, M., and T. Maruyama, 1966: Stratospheric wave disturbance propagating over the equatorial Pacific. *J. Meteor. Soc. Japan*, **44**, 291–294.